Effects of calcium buffering on glucose-induced insulin release in mouse pancreatic islets: an approximation to the calcium sensor

José A. G. Pertusa, Juan V. Sanchez-Andrés, Franz Martín* and Bernat Soria

*Departmento de Fisiología e Instituto de Bioingeniería and *Departmento de Genética, Nutrición y Toxicología e Instituto de Bioingeniería, Campus de San Juan, Universidad Miguel Hernandez, 03550 San Juan, Alicante, Spain*

1. The properties of the calcium sensor for glucose-induced insulin secretion have been studied using cell-permeant Ca^{2+} buffers with distinct kinetics and affinities. In addition, submembrane cytosolic Ca^{2+} distribution has been modelled after trains of glucose-induced action potential-like depolarizations.

2. Slow Ca^{2+} buffers (around 1 mmol l^{-1} intracellular concentration) with different affinities (EGTA and Calcium Orange-5N) did not significantly affect glucose-induced insulin release. Modelling showed no effect on cytosolic Ca^{2+} concentrations at the outermost shell (0·05 μm), their effects being observed in the innermost shells dependent on Ca^{2+} affinity.

3. In contrast, fast Ca^{2+} buffers (around 1 mmol l^{-1} intracellular concentration) with different affinities (BAPTA and Calcium Green-5N) caused a 50 % inhibition of early insulin response and completely blocked the late phase of glucose-induced insulin response, their simulations showing a decrease of $[Ca^{2+}]_i$ at both the inner and outermost shells.

4. These data are consistent with the existence in pancreatic β-cells of a higher affinity Ca^{2+} sensor than that proposed for neurons. Moreover, these data are consistent with the proposed existence of two distinct pools of granules: (i) 'primed' vesicles, colocalized with Ca^{2+} channels and responsible of the first phase of insulin release; and (ii) 'reserved pool' vesicles, not colocalized and responsible for the second phase.

It is well established that changes in the cytoplasmic Ca^{2+} concentration ($[Ca^{2+}]_i$) in pancreatic β-cells are essential for the regulation of insulin secretion (Ashcroft & Rorsman, 1989). This Ca^{2+} rise, most probably restricted to the submembrane region (Martin *et al.* 1997), promotes the fusion of the secretory granules with the plasma membrane. Aside from other effects, Ca^{2+} should interact with one or more sites located at the exocytotic machinery whose components and role have been recently identified (Kiraly-Borri *et al.* 1996; Martin *et al.* 1996; Lang *et al.* 1997).

In this regard, several components may affect the intensity and kinetics of glucose-induced insulin release. In addition to the affinity and kinetics of the Ca^{2+} sensor, the existence of a primed granule pool (Eliasson *et al.* 1997) in conjunction with steep concentration gradients (Martin *et al.* 1997) and the colocalization of the insulin secretory granule with the voltage-dependent Ca^{2+} channel (Bokvist *et al.* 1995) may condition the effect of cell-permeant exogenous Ca^{2+} buffers. The use of a new generation of Ca^{2+} buffers with known kinetic and affinity properties allows us to have indirect access to the properties of the secretory machinery.

Recent observations in other endocrine cells have demonstrated: (i) the existence of a latency between $[Ca^{2+}]_i$ and exocytosis (Chow *et al.* 1996; Eliasson *et al.* 1997); (ii) that secretion is relatively slow and continues for tens of milliseconds after Ca^{2+} entry through the voltage-dependent Ca^{2+} channels has ceased (Chow *et al.* 1996; Klingauf & Neher, 1997); and (iii) that endocrine cells have a higher Ca^{2+} sensitivity than neurones (Heinemann *et al.* 1994) and a lower maximum rate of secretion (Chow *et al.* 1994). All of these properties indicate a faint coupling of Ca^{2+} channels to the secretory machinery, with exocytosis being triggered by peaks of $[Ca^{2+}]_i$ of < 10 μmol l^{-1} at the release sites (Chow *et al.* 1994). These results contrast with those obtained from neurones (Zucker, 1996). If Ca^{2+} channels and vesicles are not strictly colocalized, then the amount of Ca^{2+} that enters during a single action potential may not be sufficient to trigger significant secretion, whereas trains of action potentials would be more effective (Zhou & Misler, 1995).

Pancreatic β-cells are unique in the sense that although they are endowed with the exocytotic and electrical machinery present in other excitable cells, the physiological trigger

promoting insulin release is a nutrient that needs to be metabolized to initiate the sequence of events that links ATP-regulated K^+ channel closure with insulin release (Ashcroft *et al.* 1984; Dunne & Petersen, 1991). It is known that in response to nutrient secretagogues, pancreatic β-cells display a series of trains of Ca^{2+} action potentials with a frequency of 2–6 Hz and a duration of 50–100 ms (Atwater *et al.* 1978). It is also accepted that: (i) these trains induce [Ca^{2+}] changes beneath the plasma membrane (Martin *et al.* 1997); (ii) pancreatic β-cells are polarized (Martin *et al.* 1997); and (iii) Ca^{2+} channels seem to be strictly colocalized with secretory vesicles (Wiser *et al.* 1999). Taking into account all these aspects, we have studied the effects of several exogenous Ca^{2+} chelators on insulin release, in order to determine how cytosolic Ca^{2+} distribution affects the dynamics of insulin exocytosis in pancreatic β-cells. In addition, we have modelled buffered Ca^{2+} diffusion in the vicinity of channels and release sites by using trains of depolarizations that resemble the ones induced by stimulatory glucose concentrations.

METHODS

Islet isolation, cell isolation and culture

Islets from adult (8- to 10-week-old) Swiss albino male mice (OF1) killed by cervical dislocation in accordance with national guidelines were isolated as previously described (Lernmark, 1974). Briefly, after pancreas digestion with collagenase (Collagenase A, Boehringer Mannheim) in a stationary bath at 37 °C, islets were separated by centrifugation and hand picked under a stereomicroscope. Once isolated, islets were dissociated into single cells in a low-calcium medium as previously described (Martin *et al.* 1997). Cells were then centrifuged, resuspended in culture medium RPMI 1640 (Sigma) supplemented with 10% fetal calf serum, penicillin (Sigma; 100 i.u. ml^{-1}), streptomycin (Sigma; 0·1 mg ml^{-1}), and 5·6 mmol l^{-1} glucose and plated on glass coverslips. Cells were kept at 37 °C in a humidified atmosphere of 95% O_2–5% CO_2 and used within 10 h of culture. Cell viability was tested by Trypan Blue exclusion (96% of the cells excluded Trypan Blue). For intracellular recording experiments, islets were isolated by microdissection as previously described (Sanchez-Andres & Soria, 1991).

Loading of islets and islet cells

Collagenase-isolated islets, microdissected islets and islet cells were incubated for 2 h at 37 °C in modified Krebs buffer supplemented with 5·6 mmol l^{-1} glucose and 3% bovine serum albumin. The medium was continuously bubbled with 95% O_2–5% CO_2 for a final pH of 7·4. Then, pancreatic islets and islet cells were loaded as previously described (Martin *et al.* 1997) with EGTA AM, BAPTA AM, Calcium Orange-5N AM, Calcium Green-5N AM, Calcium Green-1 AM, Calcium Green-2 AM, dimethylBAPTA AM, dibromoBAPTA AM and dinitroBAPTA AM (Molecular Probes) by incubation for 1 h at 37 °C in the described Krebs buffer with 100 μmol l^{-1} of these acetoxymethyl (AM) derivatives. Exogenous Ca^{2+} chelators AM were added as a concentrated stock solution in dimethyl sulphoxide (DMSO) (Sigma; final DMSO concentration 0·3% v/v). In order to facilitate the solubilization of the Ca^{2+} chelators in physiological media, the mixture also contained 10% (w/w) of the non-ionic surfactant polyol pluronic F127 (Molecular Probes). After loading, islets and cells were incubated for 1 h with the modified Krebs buffer mentioned above. The Krebs buffer was

kept at 37 °C and was constantly gassed with 95% O_2–5% CO_2 for a final pH of 7·4. Finally, Trypan Blue exclusion after cell loading was 95%.

Determination of intracellular exogenous Ca^{2+} chelator concentration

For fluorescent exogenous Ca^{2+} chelators (Calcium Green-1 AM, Calcium Green-2 AM, Calcium Orange-5N AM and Calcium Green-5N AM), 5×10^5 cells were loaded with 100 μmol l^{-1} of these AM derivatives by incubation for 1 h at 37 °C in the described Krebs buffer. Next, cells were centrifuged for 5 min at 800 *g*, washed three times and sonicated twice in 1 ml of a CaEGTA Krebs buffer (final Ca^{2+} concentration 100 nM) for 5 s using a sonic dismembrator (Artek System Corp., Farmingdale, NY, USA) at 30% maximum power. Finally, the suspension was centrifuged for 15 min at 16 700 *g* and the fluorescence emitted by the supernatant was compared to that emitted for calibration curves built with exogenous Ca^{2+} chelator (sodium salt) solutions, in the same CaEGTA Krebs buffer, at different concentrations (0, 0·1, 1, 10 and 50 μmol l^{-1}). The emitted fluorescence (531 nm for Calcium Green-1, 536 nm for Calcium Green-2, 575 nm for Calcium Orange-5N and 532 nm for Calcium Green-5N) was measured with a spectrofluorometer (model U-2000, Hitachi Ltd, Tokyo) at different excitation wavelengths depending on the exogenous Ca^{2+} chelator (488 nm for Calcium Green-5N, Calcium Green-1 and Calcium Green-2; 545 nm for Calcium Orange-5N). For non-fluorescent exogenous Ca^{2+} chelators (BAPTA AM and EGTA AM), a calibration curve of quenching of indo-1 (sodium salt)-emitted fluorescence (excitation wavelength of 360 nm and emission wavelength of 410 nm) was performed at different EGTA and BAPTA concentrations (0, 1, 10, 100 and 1000 μmol l^{-1}) in the same EGTA buffer. Then, 5×10^5 cells were loaded, centrifuged, washed and sonicated in the same manner as that used for fluorescent exogenous Ca^{2+} chelators. Finally, the quenching values of indo-1-emitted fluorescence elicited by the supernatant were extrapolated to the quenching of the indo-1 calibration curve. Cytosolic chelator concentrations were calculated from the total cell volume ($10·45 \times 10^{-7}$ l).

Electrophysiology

Membrane potential of the β-cell was recorded as previously described (Sanchez-Andres & Soria, 1991). Microdissected islets were fixed with micropins to the bottom of a 50 μl chamber and perifused at a rate of 0·8 ml min^{-1} with fresh modified Krebs buffer and constantly gassed with 95% O_2–5% CO_2 for a final pH of 7·4. Different glucose concentrations (3 and 11·1 mmol l^{-1}) were added to the superfusion medium. The test agents reached the chamber with a delay of 3 s. These delays have been corrected for in the figures. Bath temperature was maintained at 36 ± 1 °C by heating a stainless steel ring controlled by a thermostat. The temperature of the chamber was continuously monitored with a micro-thermistor. Recordings were made with an Axoclamp 2B amplifier (Axon Instruments). Data acquisition was performed with Axotape version 2.0 (Axon Instruments) and data analysis with MicroCal Origin version 3.7 (MicroCal Software, Northampton, MA, USA).

Insulin measurements

Insulin measurements were performed as previously described (Bolea *et al.* 1997). For static incubations, islets were incubated in groups of three in 1 ml of fresh modified Krebs buffer with 1% bovine serum albumin plus the different glucose concentrations (3 and 22·2 mmol l^{-1}) for 30 min at 37 °C. For islet perifusion experiments, batches of 10 islets were placed in a 50 μl chamber and perifused at a flow rate of 1 ml min^{-1} at 37 °C with fresh modified Krebs buffer with 1% bovine serum albumin plus the

Table 1. Intracellular concentrations of exogenous mobile Ca^{2+} buffers

Exogenous Ca^{2+} buffer	Cytosolic concentration (μmol l^{-1})
EGTA	853 ± 14
BAPTA	927 ± 36
Calcium Green-1	1361 ± 57
Calcium Green-2	1612 ± 63
Calcium Green-5N	1416 ± 73
Calcium Orange-5N	1280 ± 41

Data are means ± s.e.m. All determinations were run in quadruplicate. For fluorescent exogenous Ca^{2+} chelators 5×10^5 cells were loaded with 100 μmol l^{-1} of their AM derivative by incubation for 1 h at 37 °C. Then, cells were centrifuged for 5 min at 800 g, washed and sonicated in a CaEGTA buffer. The suspension was then centrifuged for 15 min at 16 700 g and the fluorescence emitted by the supernatant was compared to that emitted for calibration curves built with exogenous Ca^{2+} chelator solutions, in the same CaEGTA buffer, at different concentrations. For non-fluorescent exogenous Ca^{2+} chelators a calibration curve was performed at different EGTA and BAPTA concentrations of quenching of indo-1-emitted fluorescence in the same CaEGTA buffer. Then, 5×10^5 cells were loaded, centrifuged, washed and sonicated in the same manner as that used for fluorescent exogenous Ca^{2+} chelators. Finally, values of quenching indo-1-emitted fluorescence elicited by the supernatant were extrapolated to the quenching of the indo-1 calibration curve. Cytosolic chelator concentrations were calculated from the total cell volume.

different glucose concentrations (3 and 22·2 mmol l^{-1}). For islet cell perifusion experiments, 1×10^5 cells were packed into a 1 cm diameter column and sandwiched between two layers of swollen Sephadex G-200 microcarrier beads (Sigma). The column was perifused at a flow rate of 1 ml min^{-1} at 37 °C with fresh modified Krebs buffer with 1% bovine serum albumin plus the different glucose concentrations (3 and 22·2 mmol l^{-1}). The pancreatic islets and islet cells were first perifused in 3 mmol l^{-1} glucose for 30 min to reach a state of stable insulin release. The solutions were prewarmed at 37 °C and continuously gassed. Throughout the perifusion, effluent was continuously collected at 2 min intervals. The dead time was 2 min and has been corrected for in the figures. Both static incubation and perifused samples were kept at −20 °C until insulin determination. Insulin was assayed by radioimmuno-assay (RIA) using a kit from Diagnostic Products Corporation (Los Angeles, CA, USA). The RIA included the following steps: addition of anti-porcine insulin guinea-pig serum, incubation for 36 h at 4 °C, addition of freshly labelled ^{125}I-labelled-(Tyr A19)-human insulin, incubation for 18 h at 4 °C and precipitation of bound insulin by ethanol. Rat insulin provided by the above-mentioned kit was used to prepare the standard curves. Standard curves and samples were run in triplicate.

Statistical analysis

The results were expressed as means ± standard error of the mean (s.e.m.). For comparisons between two groups, Student's unpaired, two-tailed t test was used. *$P < 0.001$ was considered significant.

RESULTS

Intracellular concentration of exogenous mobile Ca^{2+} buffers

As demonstrated in Table 1 the estimated concentration of all permeant buffers was between 0·85 and 1·61 mmol l^{-1}. Theoretically, there may exist a limitation upon the maximum concentration of permeant chelator that can be

introduced into cells (around 1 mmol l^{-1}, as indicated in Table 1), which may be set by finite intracellular esterase activity, by active extrusion of the compound, and/or by their metabolism into inactive forms.

Effects of mobile Ca^{2+} buffers on pancreatic β-cell electrical activity

To test the possible toxicity of these permeant Ca^{2+} buffers, we studied the effects of prolonged exposure to 100 μmol l^{-1} BAPTA AM or EGTA AM on glucose-induced electrical activity. Figure 1A shows the typical pattern of electrical activity of a pancreatic β-cell stimulated with 11·1 mmol l^{-1} glucose. This shows the onset of an oscillatory activity with membrane potential oscillating between silent (hyper-polarized) and active (depolarized) phases with fast spikes (Ca^{2+} action potential) superimposed upon them. Neither EGTA (Fig. 1B) nor BAPTA (Fig. 1C) significantly modified the 11·1 mmol l^{-1} glucose-induced oscillatory pattern of electrical activity. In addition, we did not observe any inhibitory effect of EGTA or BAPTA on the fast spikes of Ca^{2+} action potential. Only a small increase, which was within the normal range for this glucose concentration, in the height of the action potentials was observed when BAPTA was used. This could be attributed to less inactivation of Ca^{2+} channels due to the presence of BAPTA. In addition, these results also indicate that electrical activity was measured in permeant Ca^{2+} buffer-loaded β-cells.

Nutrient-induced insulin release depends on mobile Ca^{2+} buffers

We have studied the effects of the forward binding constant of the Ca^{2+} buffers on 22·2 mmol l^{-1} glucose-induced insulin release, by loading the islets with diffusible exogenous buffers with different kinetic properties. Figure 2A shows

that perifused mouse islets respond to a stepwise increase in glucose concentration with a rapid and transient burst of insulin secretion (first phase) followed by a plateau (second phase) which lasted as long as glucose was present. When $100 \ \mu mol \ l^{-1}$ EGTA-loaded islets (a slow buffer with a forward binding rate (K_{on}) of $1 \cdot 5 \times 10^6 \ l \ mol^{-1} \ s^{-1}$; Smith & Miller, 1985) were perifused with $22 \cdot 2 \ mmol \ l^{-1}$ glucose no significant change in insulin release was observed (Fig. 2*B*). In addition, loading the islets with Calcium Orange-5N (a relatively slow buffer with a K_{on} of $1 \times 10^7 \ l \ mol^{-1} \ s^{-1}$; Escobar *et al.* 1997) did not affect glucose-induced insulin release either, although a small delay in the onset of the first phase was observed (Fig. 2*D*). Both EGTA and Calcium Orange-5N have a very different Ca^{2+} affinity. In fact, EGTA K_d is 200-fold less than that of Calcium Orange-5N ($0 \cdot 1$ *vs.* $20 \ \mu mol \ l^{-1}$; Smith & Miller, 1985; Escobar *et al.* 1997). On the other hand, when islets were loaded with $100 \ \mu mol \ l^{-1}$ of the very fast mobile exogenous Ca^{2+} buffers BAPTA (K_{on} of $4 \times 10^8 \ l \ mol^{-1} \ s^{-1}$; Grynkiewicz *et al.* 1985) and Calcium Green-5N (K_{on} of $1 \cdot 3 \times 10^8 \ l \ mol^{-1} \ s^{-1}$; Escobar *et al.* 1997) a markedly impaired insulin release was observed (Fig. 2*C* and *E*, respectively). As shown in Fig. 2*C* and *E*, early insulin response was 50% inhibited and late phase insulin response was completely abolished. Note that EGTA and BAPTA have a very similar Ca^{2+} affinity ($K_d = 0 \cdot 1$ and $0 \cdot 4 \ \mu mol \ l^{-1}$, respectively; Smith & Miller,

1985; Grynkiewicz *et al.* 1985). When comparing buffers with the same Ca^{2+} affinity (Calcium Orange-5N and Calcium Green-5N; $K_d = 20 \ \mu mol \ l^{-1}$; Smith & Miller, 1985) we observed that only the faster one markedly inhibited both phases of glucose-induced insulin release (Fig. 2*D* and *E*). Other fast exogenous Ca^{2+} buffers such as Calcium

Figure 2. Effects of different exogenous Ca^{2+} chelators on islet glucose-induced insulin release

Islets were loaded for 1 h at 37 °C in modified Krebs buffer with $100 \ \mu mol \ l^{-1}$ of the different exogenous chelators in AM form. Then, batches of 10 islets were perifused at a flow rate of $1 \ ml \ min^{-1}$ at 37 °C with fresh modified Krebs buffer supplemented with 1% bovine serum albumin. After a 30 min stabilization period with $3 \ mmol \ l^{-1}$ glucose, the islets were perifused for 10 min with $3 \ mmol \ l^{-1}$ glucose, then for 20 min with $22 \cdot 2 \ mmol \ l^{-1}$ glucose and finally for 10 min with $3 \ mmol \ l^{-1}$ glucose. *A*, unloaded control islets. *B*, $100 \ \mu mol \ l^{-1}$ EGTA-loaded islets. *C*, $100 \ \mu mol \ l^{-1}$ BAPTA-loaded islets. *D*, $100 \ \mu mol \ l^{-1}$ Calcium Orange-5N-loaded islets. *E*, $100 \ \mu mol \ l^{-1}$ Calcium Green-5N-loaded islets. Insulin was assayed by radioimmunoassay and determinations were run in triplicate (IRI, immunoreactive insulin). Values are expressed as means ± S.E.M. of 7 experiments. Bars represent the addition of the different glucose concentrations.
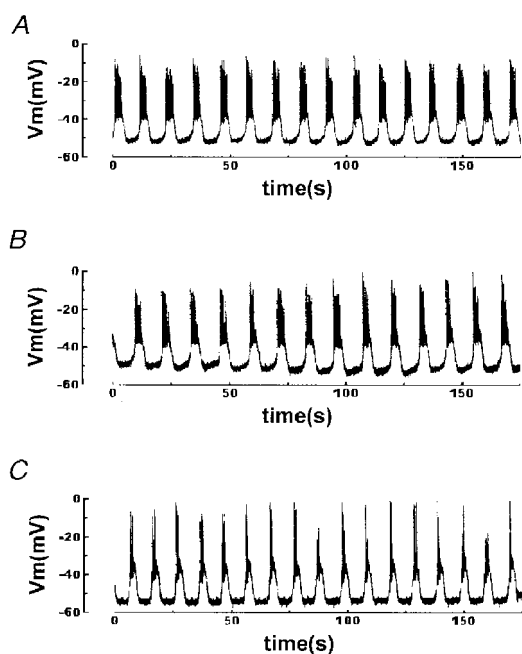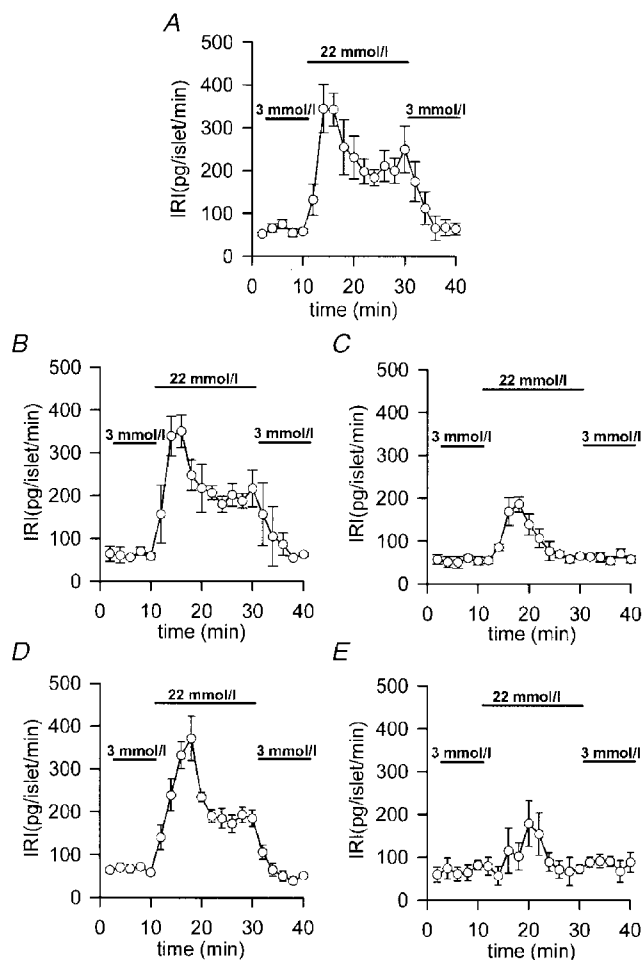
Figure 1. Effects of different exogenous Ca^{2+} chelators on glucose-induced electrical activity

Islets were loaded for 1 h at 37 °C in modified Krebs buffer with $100 \ \mu mol \ l^{-1}$ of the different exogenous chelators in AM form. The records show representative examples of the effects of $11 \cdot 1 \ mmol \ l^{-1}$ glucose on intracellularly recorded membrane potential of a pancreatic β-cell in an intact islet perifused with Krebs buffer. *A*, unloaded control islet. *B*, $100 \ \mu mol \ l^{-1}$ EGTA-loaded islet. *C*, $100 \ \mu mol \ l^{-1}$ BAPTA-loaded islet. Results are representative of 4 out of 4 cells.

Table 2. Effects of mobile Ca^{2+} buffers with different calcium affinities on glucose-induced insulin release

	IRI (pg islet^{-1} (30 min)$^{-1}$)	
	3 mmol l^{-1} glucose	22·2 mmol l^{-1} glucose
Control	376 ± 38	2587 ± 256
BAPTA	428 ± 47	1388 ± 199*
DibromoBAPTA	436 ± 35	1209 ± 240*
DimethylBAPTA	331 ± 41	1491 ± 118*
DinitroBAPTA	381 ± 53	2371 ± 343

Islets were loaded for 1 h at 37 °C in modified Krebs buffer with 100 μmol l^{-1} of the different BAPTA derivatives in AM form. Then, islets were incubated in groups of 3 in 1 ml of modified Krebs buffer with 1 % bovine serum albumin plus the different glucose concentrations (3 and 22·2 mmol l^{-1}) for 30 min at 37 °C. Insulin was assayed by radioimmunoassay and determinations were run in triplicate. Values are expressed as means ± s.e.m. *$P < 0·001$.

Green-1 and Calcium Green-2 (K_{on} of 1×10^8 l mol^{-1} s^{-1}; Escobar *et al.* 1997) elicited the same pattern of inhibition (data not shown). The inhibitory effects of high concentrations of Ca^{2+} chelators on peripherally located α-cell $[Ca^{2+}]_i$, which could be inhibiting glucagon secretion, which is very important for the insulin response of the islets, can be excluded for two reasons: (i) islet cell perifusion experiments with 100 μmol l^{-1} EGTA (Fig. 3*B*) or BAPTA (Fig. 3*C*) showed the same results as whole-islet studies; and (ii) glucagon-containing α-cell $[Ca^{2+}]_i$ oscillations disappeared when islets were exposed to high glucose concentrations (Nadal *et al.* 1999).

To further investigate the effects of mobile Ca^{2+} buffers with different calcium affinities on glucose-induced insulin

release, the effects of several BAPTA derivatives with different K_d were determined. Table 2 shows that in islet batch incubations basal insulin release (3 mmol l^{-1} glucose) was not affected by the different BAPTA derivatives after 30 min incubation. On the other hand, three of the four compounds were capable of significantly reducing 22·2 mmol l^{-1} glucose-induced insulin release (Table 2). DibromoBAPTA ($K_d = 3·6$ μmol l^{-1}; Tsien, 1980) elicited a higher reduction in insulin release (54 %). The reduced insulin release produced by dimethylBAPTA ($K_d = 0·04$ μmol l^{-1}; Tsien, 1980) was 43 %, while the reduction produced by BAPTA ($K_d = 0·1$ μmol l^{-1}) was 47 %. Finally, dinitroBAPTA ($K_d = 3 \times 10^4$ μmol l^{-1}; Pethig *et al.* 1989) did not reduce glucose-induced insulin release.

Figure 3. Effects of different exogenous Ca^{2+} chelators on isolated islet cell glucose-induced insulin release

Islet cells were loaded for 1 h at 37 °C in modified Krebs buffer with 100 μmol l^{-1} of the different exogenous chelators in AM form. Then, 1×10^5 islet cells were perifused at a flow rate of 1 ml min^{-1} at 37 °C with fresh modified Krebs buffer supplemented with 1 % bovine serum albumin. After a 30 min stabilization period with 3 mmol l^{-1} glucose, the islet cells were perifused for 10 min with 3 mmol l^{-1} glucose, then for 20 min with 22·2 mmol l^{-1} glucose and finally for 10 min with 3 mmol l^{-1} glucose. *A*, unloaded control islet cells. *B*, 100 μmol l^{-1} EGTA-loaded islet cells. *C*, 100 μmol l^{-1} BAPTA-loaded islet cells. Insulin was assayed by radioimmunoassay and determinations were run in triplicate. Values are expressed as means ± s.e.m. of 4 experiments. Bars represent the addition of the different glucose concentrations.
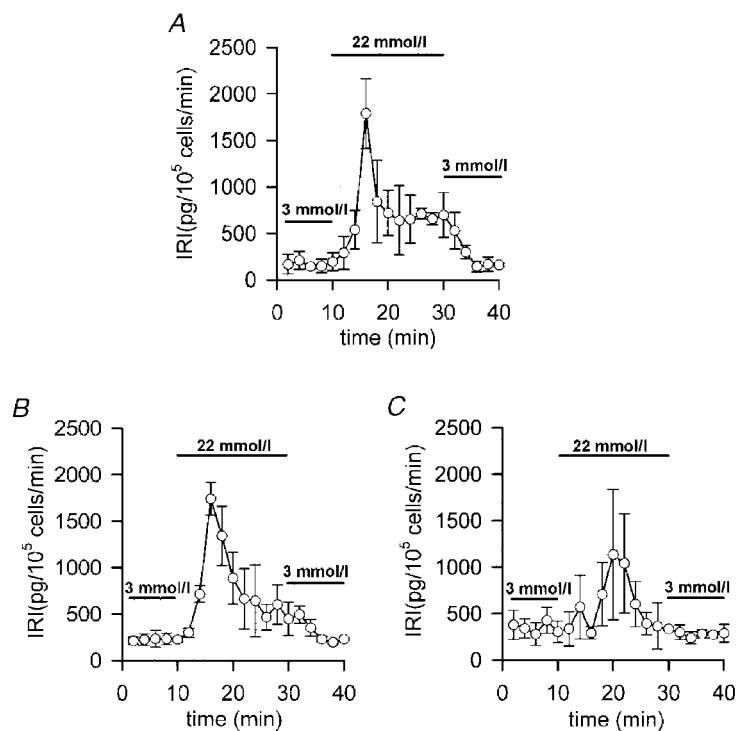
Modelling $[Ca^{2+}]_i$ signals in pancreatic β-cells loaded with mobile Ca^{2+} buffers

The simulations presented here show the complicated submembrane $[Ca^{2+}]_i$ dynamics after a rapid train of short depolarizations. Time courses were plotted of $[Ca^{2+}]_i$ for a train of 60 depolarizations (50 ms each separated by 150 ms) at different depths (0·05, 2 and 2·5 μm). Note that after 10 s the cytosolic calcium concentrations reached a steady state in all cases, thus validating the data obtained in the insulin release experiments which were carried out on a different time scale from the model. Figure 4A–E shows that in the absence of exogenous buffers and with different exogenous Ca^{2+} chelators the $[Ca^{2+}]_i$ progressively increases. More and more residual Ca^{2+} is accumulated in the innermost shells with subsequent potential-like depolarizations until a state of equilibrium is reached. The maximal cytosolic Ca^{2+} concentrations reached in the outermost shell are different in each case (with endogenous fixed buffer only, 14 μmol l^{-1}, Figs 4A and 5A; with EGTA, 13·7 μmol l^{-1}, Figs 4B and 5B; with BAPTA, 5·2 μmol l^{-1}, Figs 4C and 5C; with

Calcium Orange-5N, 5·9 μmol l^{-1}, Figs 4D and 5D; and with Calcium Green-5N, 4·4 μmol l^{-1}, Figs 4E and 5E). After finishing the potential-like depolarizations $[Ca^{2+}]_i$ drops to basal levels within a few seconds (data not shown). Running the model we observed that the concentration of fixed endogenous buffer available to bind Ca^{2+} was always higher than 130 μmol l^{-1}. For Calcium Orange-5N and Calcium Green-5N these concentrations were always higher than 1033 and 1166 μmol l^{-1}, respectively. Finally, EGTA and BAPTA are close to their saturation levels (10 and 70 μmol l^{-1}, respectively). Figures 5B and 6 show that the slow exogenous Ca^{2+} buffer EGTA did not significantly modify the $[Ca^{2+}]_i$ pattern in the different shells and the cytosolic Ca^{2+} gradient. On the other hand, the fast Ca^{2+} buffer BAPTA (Fig. 5C) lowered $[Ca^{2+}]_i$ more effectively. When we compared the effects of two low-affinity Ca^{2+} buffers ($K_d = 20$ μmol l^{-1}) with different K_{on}, such as Calcium Orange-5N (Fig. 5D) ($K_{on} = 10^7$ $l\ mol^{-1}\ s^{-1}$) and Calcium Green-5N (Fig. 5E) ($K_{on} = 10^8$ $l\ mol^{-1}\ s^{-1}$), we
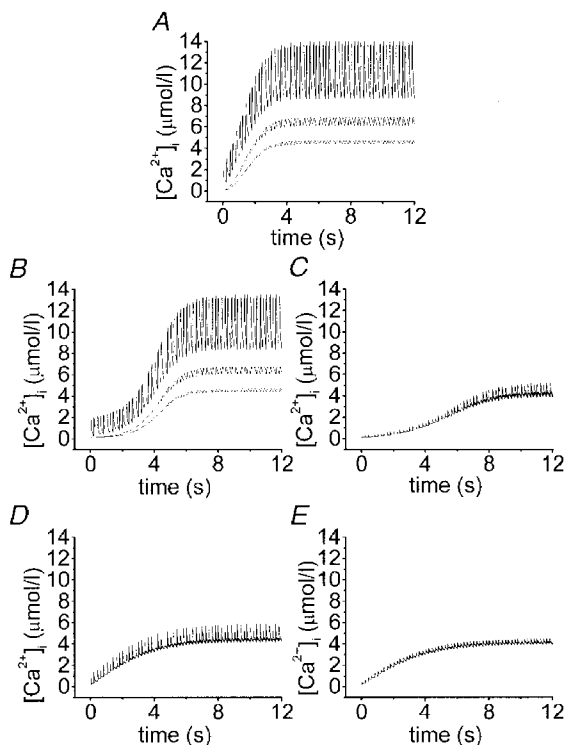

Figure 4. Effects of exogenous Ca^{2+} chelators with similar affinity and different forward binding constant on $[Ca^{2+}]_i$

Simulation of time courses of cytosolic Ca^{2+} transients for a train of 60 potential-like depolarizations (50 ms each separated by 150 ms). Different profiles in each panel correspond to Ca^{2+} transients at shells positioned 0·05 (outermost), 2·0 and 2·5 μm underneath the membrane. Other parameters are as in Table 1. In addition to the endogenous fixed buffers (A), the effects of 853 μmol l^{-1} EGTA (B), 927 μmol l^{-1} BAPTA (C), 1280 μmol l^{-1} Calcium Orange-5N (D) and 1416 μmol l^{-1} Calcium Green-5N (E) have been simulated as indicated.
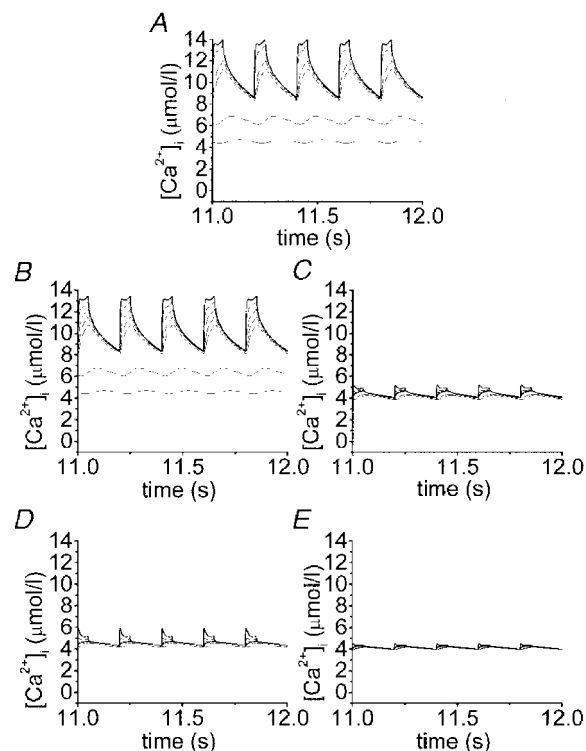

Figure 5. Detailed effects of exogenous Ca^{2+} chelators with similar affinity and different forward binding constant on $[Ca^{2+}]_i$

Simulation of time courses of cytosolic Ca^{2+} transients after reaching the steady state (last 5 pulses of a train of 60 potential-like depolarizations; 50 ms each separated by 150 ms). Different profiles in each panel correspond to Ca^{2+} transients at shells positioned 0·05 (outermost, represented as bold trace), 0·2, 0·4, 0·6, 0·8, 2·0 and 2·5 μm beneath the membrane. Other parameters are as in Table 1. In addition to the endogenous fixed buffers (A), the effects of 853 μmol l^{-1} EGTA (B), 927 μmol l^{-1} BAPTA (C), 1280 μmol l^{-1} Calcium Orange-5N (D) and 1416 μmol l^{-1} Calcium Green-5N (E) have been simulated as indicated.

observed that whereas Calcium Green-5N (Fig. 5*E*) (fast buffer) almost completely removed the cytosolic Ca^{2+} gradient near the cell membrane (see 0·05–0·5 μm shells) (Figs 5*E* and 6), Calcium Orange-5N (slow buffer) still permitted a significant Ca^{2+} gradient (Figs 5*D* and 6).

DISCUSSION

Experiments involving capacitance measurements of exocytosis and photorelease of Ca^{2+} enabled Eliasson *et al.* (1997) to estimate the delay between elevation of $[Ca^{2+}]_i$ and fusion of the granular membrane with the plasma membrane between <17 and 45 ms in pancreatic β-cells. Such behaviour can be described in other ways if one assumes that before any stimulation a small number of secretory vesicles are already docked very close to the membrane and the rest of them are located at approximately a 300 nm distance. Due to the fact that neuroendocrine cells have significant amounts of endogenous fixed Ca^{2+} buffers which tend to prolong $[Ca^{2+}]_i$ transients, the time course of the Ca^{2+} and the resulting delay is expected to be highly dependent upon the relative amount of endogenous fixed Ca^{2+} buffer (Sala & Hernandez-Cruz, 1990). We have therefore tested the effects of increasing mobile Ca^{2+} buffers on glucose-induced insulin release and modelled their effects on the Ca^{2+} signal near the plasma membrane.

An estimate of intracellular buffer concentration is required to compare the action of different buffers and predict their probable effects on calcium concentrations and insulin release. Our observations show that pancreatic β-cells have a cytoplasmic chelator accumulation of around 1 mmol l^{-1}, close to the maximum limit of permeant chelator that can be introduced into cells (Tsien, 1981). These data suggest that the approximations used to determine buffer concentrations are reasonable. Another problem is that the insulin release and the $[Ca^{2+}]_i$ effects of permeant Ca^{2+} buffers can be attributable to the hydrolysed AM ester moiety. In addition, other mechanisms of chelator action cannot be excluded. These could include the direct pharmacological effects of the chelators or their by-products and reduction of the resting $[Ca^{2+}]_i$ to levels in the order of 10^{-9} mol l^{-1}. The fact that after Ca^{2+} buffer loading, glucose-induced electrical activity and insulin release are conserved, even in dinitroBAPTA-loaded islets (a very low Ca^{2+}-affinity buffer), indicates that pancreatic β-cell metabolism, ATP-regulated K^+ channels, Ca^{2+}-dependent action potentials and exocytotic machinery are operative in the physiological range. In addition, it suggests that cellular homeostatic mechanisms can maintain resting $[Ca^{2+}]_i$ at a 'set point' near normal levels despite the presence of high amounts of exogenous calcium buffer.

It has been demonstrated that a step increase in $[Ca^{2+}]_i$ elicits a fast ATP-independent component of capacitance increase and a slowly developing ATP-dependent component (Eliasson *et al.* 1997). It was suggested that these components are the single cell counterparts of the first and second phase

of insulin secretion (Grodsky, 1994). This reflects the existence of at least two functionally distinct pools of granules: first, the 'readily releaseable' or 'primed' pool; second, the 'reserve' pool. As observed, whereas fast mobile exogenous Ca^{2+} buffers completely blocked the second phase and partially affected the first phase, slow mobile exogenous Ca^{2+} buffers did not modify any phase of glucose-induced insulin release. That is to say, whereas fast Ca^{2+} buffers completely block the mobilization of granules from the reserve pool into the readily releasable pool, slow buffers did not affect this mobilization. According to the results, fast Ca^{2+} buffers (BAPTA and Calcium Green-5N) should partially block the exocytosis of granules which have reached the ultimate station before the final Ca^{2+}-dependent step, the primed vesicles (first phase), which should be located in close proximity to Ca^{2+} channels; and should block the mobilization of the reserve pool of vesicles, not colocalized with Ca^{2+} channels and placed at approximately a 300 nm distance, as predicted by the model. In the simulations we observed the slow Ca^{2+} buffer Calcium Orange-5N decreasing $[Ca^{2+}]_i$ at innermost shells (farther away than 400 nm), whereas fast buffers (BAPTA and Calcium Green-5N) decreased $[Ca^{2+}]_i$ mostly at outer (beyond 50 nm) shells and to the same extent as slow buffers in the innermost shells. Thus, we suggest that the first phase of glucose-induced insulin release is due to exocytosis of a primed pool of secretory granules located in close proximity to Ca^{2+} channels (around 50 nm), whereas the
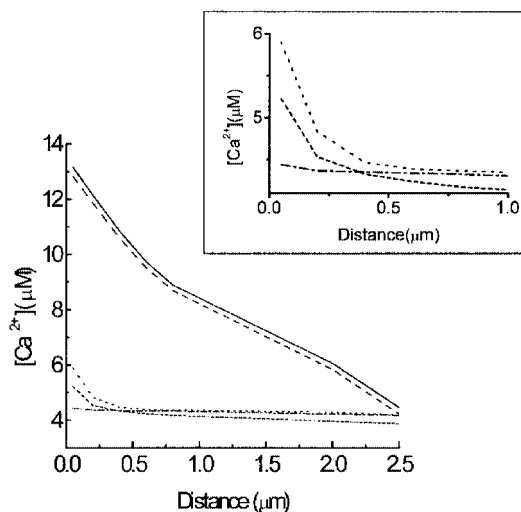

Figure 6. Computer simulation of the effects of exogenous Ca^{2+} chelators on $[Ca^{2+}]_i$ gradients within a β-cell at various distances from the plasma membrane

Simulation of cytosolic Ca^{2+} gradients built during the last Ca^{2+} transient after a train of 60 potential-like depolarizations. In addition to the endogenous fixed buffer (continuous line), the effects of 853 μmol l^{-1} EGTA (dashed line), 927 μmol l^{-1} BAPTA (short-dashed line), 1280 μmol l^{-1} Calcium Orange-5N (dotted line) and 1416 μmol l^{-1} Calcium Green-5N (dashed-dotted line) on submembrane $[Ca^{2+}]_i$ gradient have been simulated as indicated. Inset, detailed $[Ca^{2+}]_i$ gradients in the first micrometre from the plasma membrane.

second phase is due to mobilization of a reserve pool of granules placed at approximately 300 nm from the plasma membrane.

In pancreatic β-cells, it appears that $[Ca^{2+}]_i$ at secretory sites reaches 7 μmol l^{-1} during depolarization (Bokvist *et al.* 1995) and around 2 μmol l^{-1} during glucose stimulation (Martin *et al.* 1997). The model also predicts a $[Ca^{2+}]_i$ in the outermost shells not higher than 14 μmol l^{-1}. This apparent difference could be due to an underestimation of $[Ca^{2+}]_i$ caused by Ca^{2+} imaging techniques which do not allow measurements in close proximity to the plasma membrane.

Finally, fast Ca^{2+} buffers with low affinity, like the BAPTA derivative dinitroBAPTA ($K_d = 3 \times 10^4$ μmol l^{-1}), did not inhibit glucose-induced insulin release. Note that dinitroBAPTA itself reduced transmitter release in the presynaptic terminal of the giant squid synapse by 27 % (Adler *et al.* 1991). On the other hand, the fast Ca^{2+} buffer dibromoBAPTA ($K_d = 3\cdot6$ μmol l^{-1}) was the most efficient at inhibiting glucose-induced insulin release. All these data suggest that the Ca^{2+} receptor that initiates release does not need to have such a low affinity for Ca^{2+} as is the case in neurons.

In conclusion, these results provide additional evidence in favour of the existence of two different vesicle types responsible for glucose-induced insulin release: (i) primed vesicles, located very close to the Ca^{2+} channels and (ii) reserve vesicles, not strictly colocalized with the Ca^{2+} channels. Due to the fact that the second phase of glucose-induced insulin release may last for longer periods (from minutes to hours), it can be assumed that the speed of secretion is usually not so critical for pancreatic β-cell function. Moreover a low affinity Ca^{2+} sensor would require very high $[Ca^{2+}]_i$ for hours, a condition which is not compatible with cell survival.

APPENDIX

Computational model

The model takes into account several different species, namely Ca^{2+} and either of two buffer systems (B_1, B_2) in both their free and Ca^{2+}-bound forms. The characteristics of B_1 were chosen to mimic endogenous fixed buffers (Thomas *et al.* 1990; Neher & Augustine, 1992). B_2 represents an exogenous Ca^{2+} buffer and its characteristic change depending on buffer characteristics modelled. The partial differential equation describing diffusion for all species can be written as (Crank, 1975):

$$\partial[S]/\partial t = D_s[(\partial^2[S]/\partial r^2) + (2/r)(\partial[S]/\partial r)], \qquad (A1)$$

where [S] is the concentration of diffusible species, r is the radial distance and D_s is the diffusion coefficient of the diffusible species.

The model is composed of 50 concentric shells of uniform thickness, $\delta = 50$ nm. The diffusional properties of each shell are considered to exist only at the shell interfaces and are represented as a set of rate constants between shell surface limits. Diffusional distance (shell thickness), and diffusion coefficients are taken into account. The result of this assumption is that for the ith of n shells eqn (A1) becomes:

$$(d[S]_i/dt)_{di} = D_s/V_i\,\delta\,(A_{i-1}\,([S]_{i-1} - [S]_i) - A_i([S]_i - [S]_{i+1})),$$

$$(A2)$$

where $[S]_i$ is the concentration of the diffusible species (Ca^{2+} or a diffusible buffer), di is the effect of the diffusion of the diffusible species, D_s is the diffusion coefficient of the diffusible species, δ is the shell thickness, and V_i is the shell volume. A_{i-1} and A_i are, respectively, the surface areas of the outer and inner spherical boundaries of the ith shell. To solve this equation, initial and boundary conditions must be defined. All species are initially assumed to be homogeneously distributed throughout the cell with known total concentrations of each buffer and initial calcium. Given the equilibrium constants (K_d) for the three buffers, the initial concentrations of bound and unbound Ca^{2+} buffers can be easily calculated according to the mass-action law for each individual case. The boundary conditions specify that diffusion does not occur across the outermost spherical boundary or out of the innermost sphere. Thus, A_{i-1} is set to zero for the first (outermost) shell, while A_i is set to zero for the nth (innermost) shell.

The effect of buffering on concentration of the different species (B_1, B_2 and Ca^{2+}) is represented by:

$$(d[C]_i/dt)_{Bi} = k_{off}\,[CB]_i - k_{on}\,[C]_i\,[B]_i, \qquad (A3)$$

where $[C]_i$ is the concentration of free Ca^{2+}, Bi is the effect of the Ca^{2+} binding, $[B]_i$ is the concentration of the unbound buffer, $[CB]_i$ is the concentration of bound buffer and finally, k_{off} and k_{on} are, respectively, the reverse and forward rate constant of the binding reaction.

Active extrusion of Ca^{2+} out of the spherical model from the first shell is defined according to Michaelis-Menten kinetics (Sala & Hernandez-Cruz, 1990). This system is described by the following equation:

$$(d[C]/dt)_{Ex} = -V_{max}A[C]/V([C] + K_m), \qquad (A4)$$

where Ex is the effect of the Ca^{2+} extrusion, V_{max} is the maximal speed of transport, A is the area of the cell, V is the volume of the outermost shell, [C] is the concentration of Ca^{2+} in the outermost shell and K_m is the half-maximal activating concentration. As noted by Sala & Hernandez-Cruz (1990), a steady leakage of calcium into the outermost shell is needed to maintain a fixed $[Ca^{2+}]_i$ at rest. This leak is thus constant and defined by eqn (A4) with the exception that the concentration of Ca^{2+} used equals the initial 'intracellular' Ca^{2+} concentration ($0\cdot1$ μmol l^{-1}, see Table 1).

The rate of change of free Ca^{2+} due to influx in the first (outermost) shell is defined by:

$$(d[C]/dt)_{In} = I_{Ca}/2FV, \qquad (A5)$$

where In is the effect of the inward Ca^{2+} curent on the first shell, I_{Ca} is the inward Ca^{2+} current, F is Faraday's constant, and V is the volume of the first shell. I_{Ca} was fitted to an exponential decay whose values decreased from 250 pA to 41 pA; a similar Ca^{2+} current was evoked by Bokvist *et al.* (1995) by a 50 ms depolarization in pancreatic islet cells. In all cases, we used a series of 60 consecutive depolarizations, lasting 50 ms, separated by 150 ms silent phases.

The effect of calcium-transporting ATPase flux into the ER lumen in the last shell (innermost shell) was described by Saleet *et al.* (1992):

$$(d[C]/dt)_{ER} = -K_{pump}[C], \tag{A6}$$

where ER is the effect of Ca^{2+} uptake by endoplasmic reticulum, K_{pump} is the rate constant of ATPase and [C] is the concentration of Ca^{2+} in the innermost shell.

Table 3. Parameters used for simulations

Symbol	Definition	Standard value	Comment
Geometry			
R	Cell radius	5 μm	Cell size of a pancreatic β-cell
δ	Shell thickness	0·05 μm	
Calcium			
I_{Ca}	Whole-cell current	250–41 pA	Fitted to an exponential decay whose values decreased from 250 pA to 41 pA, Bokvist *et al.*(1995)
$[C]_i$	Basal calcium concentration	0·1 μmol l^{-1}	
D_s	Diffusion constant for free Ca^{2+} in cytoplasm	2×10^{-6} cm^2 s^{-1}	Values used by Nowycky & Pinter (1993)
Calcium extrusion			
V_{max}	Maximum velocity of transport	2 pmol cm^{-2} s^{-1}	Sala & Hernandez-Cruz (1990)
K_m	Michaelis-Menten constant	0·83 μmol l^{-1}	Sala & Hernandez-Cruz (1990)
Endoplasmic reticulum			
K_{pump}	Pump rate into the endoplasmic reticulum	300 s^{-1}	Estimated from values used for sarcoplasmic reticulum by Ogawa *et al.*(1981)
Endogenous buffers			
Fixed buffer			
$[B_2]$	Total concentration	500 μmol l^{-1}	Nowycky & Pinter (1993)
K_d	Dissociation constant	5 μmol l^{-1}	Nowycky & Pinter (1993)
K_{on}	Forward binding rate	1×10^8 l mol^{-1} s^{-1}	Nowycky & Pinter (1993)
Exogenous buffers			
D_s	Diffusion constant for free and Ca^{2+}-bound buffers in cytoplasm	2×10^{-6} cm^2 s^{-1}	Nowycky & Pinter (1993)
EGTA			
$[B_3]$	Total concentration	853 μmol l^{-1}	Our estimated value
K_d	Dissociation constant	0·1 μmol l^{-1}	Measured at Molecular Probes
K_{on}	Forward binding rate	$1·5 \times 10^6$ l mol^{-1} s^{-1}	Smith & Miller (1985)
BAPTA			
$[B_3]$	Total concentration	927 μmol l^{-1}	Our estimated value
K_d	Dissociation constant	0·4 μmol l^{-1}	Measured at Molecular Probes
K_{on}	Forward binding rate	4×10^8 l mol^{-1} s^{-1}	Grynkiewicz *et al.* (1985)
Calcium Orange-5N			
$[B_3]$	Total concentration	1280 μmol l^{-1}	Our estimated value
K_d	Dissociation constant	20 μmol l^{-1}	Measured at Molecular Probes
K_{on}	Forward binding rate	1×10^7 l mol^{-1} s^{-1}	Escobar *et al.* (1997)
Calcium Green-5N			
$[B_3]$	Total concentration	1416 μmol l^{-1}	Our estimated value
K_d	Dissociation constant	20 μmol l^{-1}	Measured at Molecular Probes
K_{on}	Forward binding rate	$1·3 \times 10^8$ l mol^{-1} s^{-1}	Escobar *et al.* (1997)
Time increment			
Δt		2 μs	

Finally, the following equations (by combining eqns (2)–(6)) describe the change in the concentration for each diffusible species involved in each shell:

$$d[B_i]/dt = (d[C]_i/dt)_{B1}, \tag{A7}$$

$$d[B_2]/dt = (d[B_2]_i/dt)_{di} + (d[C]_i/dt)_{B2}, \tag{A8}$$

$$d[CB_1]/dt = -(d[C]_i/dt)_{B1}, \tag{A9}$$

$$d[CB_2]/dt = (d[CB_2]_i/dt)_{di} - (d[C]_i/dt)_{B2}, \tag{A10}$$

$$d[C]_i/dt = (d[C]_i/dt)_{di} + (d[C]_i/dt)_{B1} + (d[C]_i/dt)_{B2}$$
$$+ (d[C]/dt)_{ER} + (d[C]/dt)_{Ex} + (d[C]/dt)_{Leak} + (d[C]/dt)_{In}. \tag{A11}$$

The ER term in eqn (A11) take values different from zero only at the innermost shell and the last three terms take a zero value in all shells except in the outermost shell.

Equations (A7)–(A11) were integrated using the first-order Euler algorithm. The simulations were run on a PC-compatible computer with a program written in Labview. The parameters used in the model are indicated in Table 3.

ADLER, E. M., AUGUSTINE, G. J., DUFFY, S. N. & CHARLTON, M. P. (1991). Exogenous intracellular calcium chelators attenuate neurotransmitter release at the squid giant synapse. *Journal of Neuroscience* **11**, 1496–1507.

ASHCROFT, F. M., HARRISON, D. E. & ASHCROFT, S. J. H. (1984). Glucose induces closure of single potassium channels in isolated rat pancreatic β-cells. *Nature* **312**, 446–448.

ASHCROFT, F. M. & RORSMAN, P. (1989). Electrophysiology of the pancreatic β-cell. *Progress in Biophysics and Molecular Biology* **54**, 87–143.

ATWATER, I., RIBALET, B. & ROJAS, E. (1978). Cyclic changes in potential resistance of the β-cell membrane induced by glucose in islets of Langerhans from mouse. *Journal of Physiology* **278**, 117–139.

BOKVIST, K., ELIASSON, L., ÄMMÄLÄ, C., RENSTRÖM, E. & RORSMAN, P. (1995). Colocalization of L-type Ca²⁺ channels and insulin-containing secretory granules and its significance for the initiation of exocytosis in mouse pancreatic β-cell. *EMBO Journal* **14**, 50–57.

BOLEA, S., PERTUSA, J. A. G., MARTIN, F., SANCHEZ-ANDRES, J. V. & SORIA, B. (1997). Regulation of pancreatic β-cell electrical activity and insulin release by physiological amino acid concentrations. *Pflügers Archiv* **433**, 699–704.

CHOW, R. H., KLINGAUF, J., HEINEMANN, C., ZUCKER, R. S. & NEHER, E. (1996). Mechanisms determining the time course of secretion in neuroendocrine cells. *Neuron* **16**, 369–376.

CHOW, R. H., KLINGAUF, J. & NEHER, E. (1994). Time course of Ca²⁺ concentration triggering exocytosis in neuroendocrine cells. *Proceedings of the National Academy of Sciences of the USA* **91**, 12765–12769.

CRANK, J. (1975). Diffusion in a sphere. In *The Mathematics of Diffusion*, ed. CRANK, J., pp. 89–103. Clarendon Press, Oxford.

DUNNE, M. J. & PETERSEN, O. H. (1991). Potassium selective ion channels in insulin-secreting cells: physiology, pharmacology and their role in stimulus secretion coupling. *Biochimica et Biophysica Acta* **1071**, 67–82

ELIASSON, L., RENSTRÖM, E., DING, W. J., PROKS, P. & RORSMAN, P. (1997). Rapid ATP-dependent priming of secretory granules precedes Ca²⁺-induced exocytosis in mouse pancreatic β-cells. *Journal of Physiology* **503**, 399–412.

ESCOBAR, A. L., VELEZ, P., KIM, A. M., CIFUENTES, F., FILL, M. & VERGARA, J. L. (1997). Kinetic properties of DM-nitrophen and calcium indicators: rapid and transient response to flash photolysis. *Pflügers Archiv* **434**, 615–631.

GRODSKY, G. M. (1994). An update on implications of phasic insulin secretion. In *Frontiers of Insulin Secretion and Pancreatic β-Cell Research*, ed. FLATT, P. & LENZEN, S., pp. 421–430. Smith-Gordon, London.

GRYNKIEWICZ, G., POENIE, M. & TSIEN, R. Y. (1985). A new generation of Ca²⁺ indicators with greatly improved fluorescence properties. *Journal of Biological Chemistry* **260**, 3340–3350.

HEINEMANN, C., CHOW, R. H., NEHER, E. & ZUCKER, R. J. (1994). Kinetics of the secretory response in bovine chromaffin cells following flash photolysis of caged Ca²⁺. *Biophysical Journal* **67**, 546–557.

KIRALY-BORRI, C., MORGAN, A., BURGOYNE, R., WELLER, U., WOLLHEIM, C. & LANG, J. (1996). Soluble N-ethylmaleimide sensitive factor attachment protein and N-ethylmaleimide insensitive factors are required for Ca²⁺ stimulated exocytosis of insulin. *Biochemical Journal* **314**, 199–223.

KLINGAUF, J. & NEHER, E. (1997). Modeling buffered Ca²⁺ diffusion near the membrane: implications for secretion in neuroendocrine cells. *Biophysical Journal* **72**, 674–690.

LANG, J., ZHANG, H., VAIDYANATHAN, V. V., SADOUL, K., NIEMANN, H. & WOLLHEIM, C. B. (1997). Transient expression of botulinum neurotoxin C1 light chain differentially inhibits calcium and glucose induced insulin secretion in clonal β-cells. *FEBS Letters* **419**, 13–17.

LENMARK, A. (1974). The preparation of, and studies on, free cell suspensions from mouse pancreatic islets. *Diabetologia* **10**, 431–438.

MARTIN, F., RIBAS, J. & SORIA, B. (1997). Cytosolic Ca²⁺ gradients in pancreatic islet cells stimulated by glucose and carbachol. *Biochemical and Biophysical Research Communications* **235**, 465–468.

MARTIN, F., SALINAS, E., VAZQUEZ, J., SORIA, B. & REIG, J. A. (1996). Inhibition of insulin release by synthetic peptides shows that the H3 region at the C-terminal domain of syntaxin-1 is crucial for Ca²⁺- but not for guanosine 5′-[γ-thio]triphosphate-induced secretion. *Biochemical Journal* **320**, 201–205.

NADAL, A., QUESADA, I. & SORIA, B. (1999). Homologous and heterologous asynchronicity between identified α, β and δ cells within intact islets of Langerhans. *Journal of Physiology* **517**, 85–93.

NEHER, E. & AUGUSTINE, G. J. (1992). Calcium gradients and buffers in bovine chromaffin cells. *Journal of Physiology* **450**, 273–301.

NOWYCKY, M. C. & PINTER, M. J. (1993). Time course of calcium and calcium-bound buffers following calcium influx in a model cell. *Biophysical Journal* **64**, 77–91.

OGAWA, Y., KUREBAYASHI, N., IRIMAJIRI, A. & HANAI, T. (1981). Transient kinetics for calcium uptake by fragment sarcoplasmic reticulum from bullfrog skeletal muscle with reference to the rate of relaxation in living muscle. *Advances in Physiological Science* **5**, 417–435.

PETHIG, R. R., KUHN, M., PAYNE, R., ADLER, E. M., CHEN, T. H. & JAFFE, L. F. (1989). On the dissociation constants of BAPTA-type calcium buffers. *Cell Calcium* **10**, 491–498.

SALA, F. & HERNANDEZ-CRUZ, A. (1990). Calcium diffusion modeling in a spherical neuron. Relevance of buffering properties. *Biophysical Journal* **57**, 313–324.

SALEET, M., VAJDA, S., PASIK, P. & GILLO, B. (1992). A membrane model for cytosolic calcium oscillations. A study using *Xenopus* oocytes. *Biophysical Journal* **63**, 235–246.

SANCHEZ-ANDRES, J. V. & SORIA, B. (1991). Muscarinic inhibition of the pancreatic β-cell. *European Journal of Pharmacology* **205**, 89–91.

SMITH, G. L. & MILLER, D. J. (1985). Potentiometric measurements of stoichiometric and apparent affinity constants of EGTA for protons and divalent ions including calcium. *Biochimica et Biophysica Acta* **839**, 287–299.

THOMAS, P., SURPRENANT, A. & ALMERS, W. (1990). Cytosolic Ca^{2+}, exocytosis, and endocytosis in single melanotrophs of the rat pituitary. *Neuron* **5**, 723–733.

TSIEN, R. Y. (1980). New calcium indicators and buffers with high selectivity against magnesium and protons: design, synthesis and properties of prototype structures. *Biochemistry* **19**, 2396–2404.

TSIEN, R. Y. (1981). A non-disruptive technique for loading calcium buffers and indicators into cells. *Nature* **290**, 527–528.

WISER, O., TRUS, M., HERNANDEZ, A., RENSTRÖM, E., BARG, S., RORSMAN, P. & ATLAS, D. (1999). The voltage sensitive Lc-type Ca^{2+} channel is functionally coupled to the exocytotic machinery. *Proceedings of the National Academy of Sciences of the USA* **96**, 248–253.

ZHOU, Z. & MISLER, S. (1995). Action potential-induced quantal secretion of catecholamines from rat adrenal chromaffin cells. *Journal of Biological Chemistry* **270**, 3498–3505.

ZUCKER, R. J. (1996). Exocytosis: A molecular and physiological perspective. *Neuron* **17**, 1049–1055.

Corresponding author

B. Soria: Department of Physiology and Institute of Bioengineering, School of Medicine, Campus de San Juan, 03550 San Juan de Alicante, Spain.

Email: bernat.soria@umh.es